School of Mathematical
and Physical Sciences

University of

Department of Mathematics and Statistics

Preprint MPS-2013-03

2 May 2013

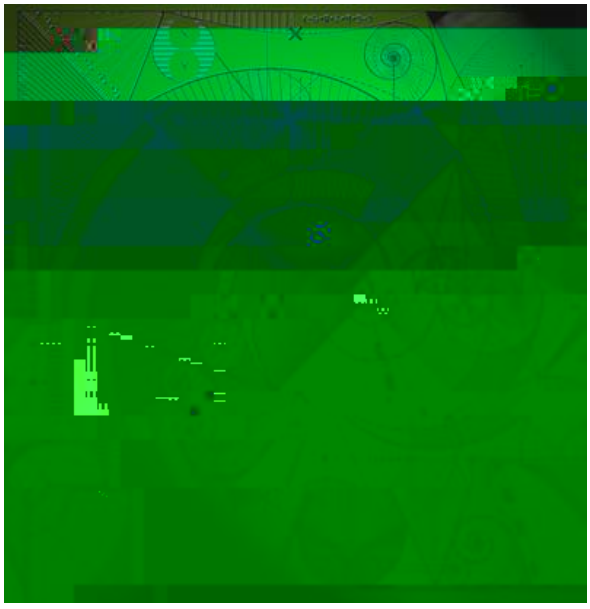

Primary Evolving Networks and the Comparative Analysis of Robust and Fragile Structures

Peter Grindrod, Zhivko Stoyanov and Garry Smith

May 2, 2013

Abstract

When evolving networks are very large (in terms of the number of vertices) there is usually some need to summarize those networks. Here we introduce the

Q

then then M insults have had little impact on the primary network, which must consequently be relatively large. If this is large then the M insults have removed a more significant amount of functionality and the primary network must consequently be relatively small.

Next consider the successive fractional losses,

$$\left\{ \frac{Q_{j-1} - Q_j}{Q_0 - Q_M} | j = 1, \ldots, M \right\},$$

and suppose that they are sorted into descending order. Then we may plot the cumulative fraction of total loss against the cumulative fraction of the total knockouts (ordered by descending size of loss), see Fig. 1. This curve lies within the unit square, connecting $(0,0)$ to $(1,1)$, above the diagonal with a negative second derivative. We shall calculate the area under this (ROC-like) curve. It is equal to one half if and only if all of the fractional losses are equal (all knock-outs produce the same loss). Il f73sll 4035254(l)- ,390954o9525.746867468(r(s)7604993(o)-303.012I)19268.63(g)-53(x468(a

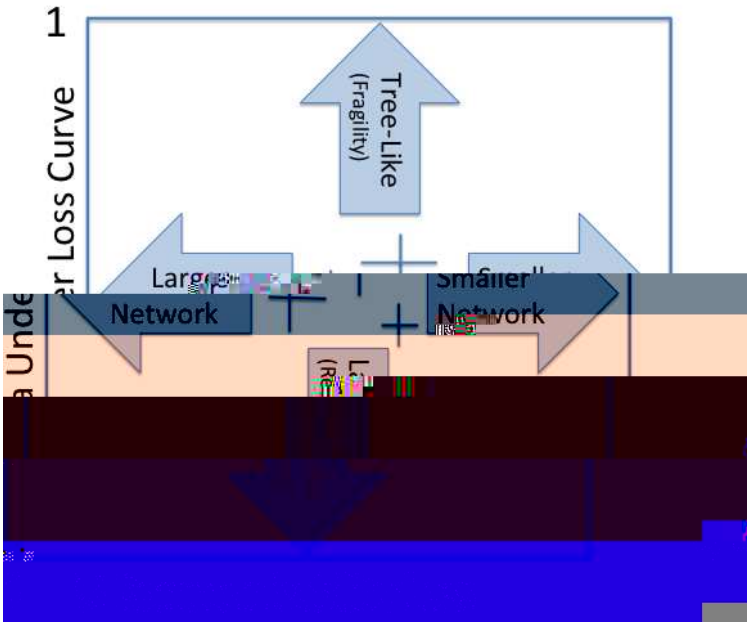

Figure 2: Three primary networks plotted as estimates and two sided ranges, with respect to both performance measures.

3 Primary networks for fMRI brain scan data

We consider data from an fMRI scan of a human brain, which contains around $n = 2.5 \times 10^5$ voxels (small three dimensional volumes within which activity can be measured), which we shall treat as vertices. Here a_{ij} represents a one-sided covariance of the measured activities (transient blood oxygen level which is related to energy usage) within voxels v_i and v_j, over 10 successive time frames (from the scan). We step the 10-frame window through a full set of 110 time frames, producing an evolving weighted network over $K = 11$ discrete time steps, as a sequence of such

we may see those regions of the brain, voxel by voxel, for which **b** dominates **r**: that is, they have *more* downstream paths than upstream paths, coloured red in Fig. 3. Similarly, those voxels for which **r** dominates **b**: that is, they have *more* upstream paths than downstream paths, which are coloured green in Fig. 3.

Clearly these dynamics paths (representing successive chains of events carrying over at least two time-steps) yield a highly structured field. Moreover, if we randomly permute all of the time-steps (permute the A_k's) and then repeat the whole operation, the resulting differences, $\mathbf{b}-\mathbf{r}$, become much smaller. Such a permutation can be carried through to show this field observed within the unpermuted data is highly statistically significant. So the dynamical information extracted confidently reflects some sorts of processes that are actually taking place and is not simply an artifact of the observations or the method. The structures in Fig. 3 themselves are intersting too. They have relatively short wavelength and display clear striping throughout the cortex.

Scientists working in the fMRI brain scan field may have never encountered striping like this either because they are in the habit of defining static networks, where the communicability (centrality) matrix is symmetric and hence $\mathbf{b}=\mathbf{r}$, or else of analyzing the data at lower resolutions. A common reaction is to declare that this is *merely noise*, presumably because it shows evidence of dynamic structure within regions that they typically wish to "parcellate", and is an *inconvenient* phenomenon. In fact these patterns are very far from being spatial noise indeed, and they have a very distinctive scale. Our permutation tests also show that the patterning is not the result of temporal noise: these patterns represent dynamical flows form small scale volumes behaving as relative sources and relative sinks for inter-brain communication.

The resulting distributions for $\mathbf{b}=(b_1,...,b_n)^T$ and $\mathbf{r}=(r_1,...,r_n)^T$ are shown in Fig. 4. From these we select threshold values of β and ρ so as to retain the upper modes within the primary network. This means that approximately half the vertices (1.25×10^5) are retained within V.

Using this approach, we have analysed 967 separate fMRI scans, which are part of the data available from the 1000 Connectome Project[1]. The multimodal structure in these distributions is similar in all cases: so it is straightforward to select a primary network containing about half of the voxels.

Next we recalculate the measures associated with the primary network's communicability matrix, Q. In Fig. 5 we show the values obtained in **b** versus those in **b**; and the values obtained in **r** versus those in **r**. Since the primary network is dominant within the full communicability matrix, by construction, these are very closely correlated.

To visualize the resulting primary network on the reduced set of vertices, V, consider the field given by the source communicability, the row sums, **b**. This is shown in Fig. 6. Notice that the left and right hemispheres have now become mostly separated within the primary network and there are some voids within the brain mass. The most extreme positive **b**-values are towards the outside layers of the cortex.

Next we apply the method given in section 2.3 to consider an ensemble of 967 fMRI brains scans. These are all scans of resting brains, from a number of laboratories, and each has been downloaded from the connectime database and then normalized (mapped onto a standard voxelated representation). We also restricted each normalized scan to 110 time frames, and thus $K=11$

[1]For more information visit http://fcon_1000.projects.nitrc.org/ or http://www.nitrc.org/.

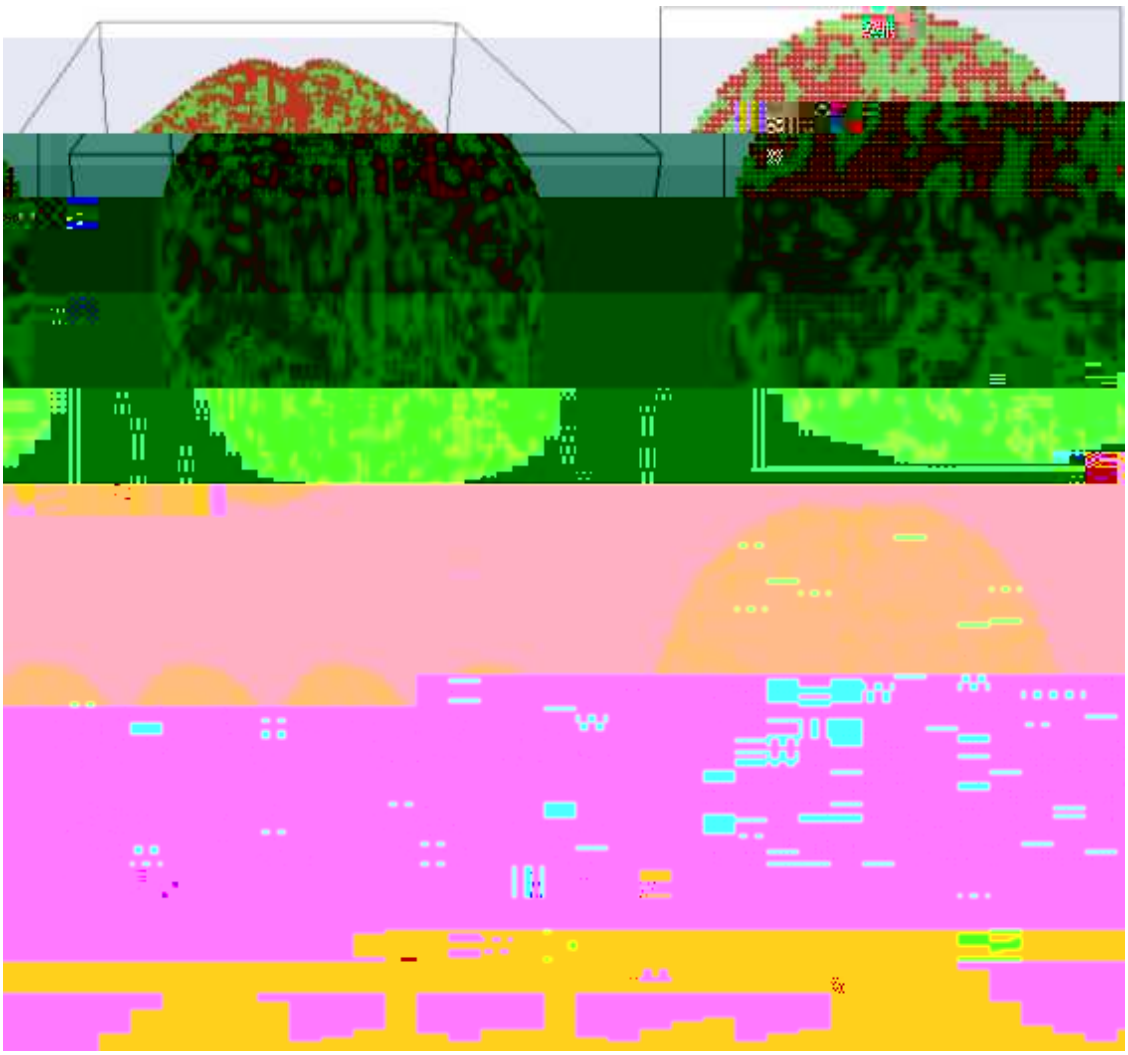

Figure 3: A 3D map of a brain obtained from the source minus sink scores, $\mathbf{b} - \mathbf{r}$.

timesteps.

For each brain we procceeded independently as follows:

(a) we identified the primary network using suitable threshold parameters $(\beta\ ,\rho\ )$;

(b) we calculated Q and its related measures (and tests);

(c) we degraded the primary network with $M = 1000$ successive voxel knock-outs;

(d) we repeated step (c) independently 100 times to estimate means and ranges for the two performance measures.

This process involved making around 100 000 separate communicability calculations for original and degraded primary networks; each of which, conceptually at least, was made based on

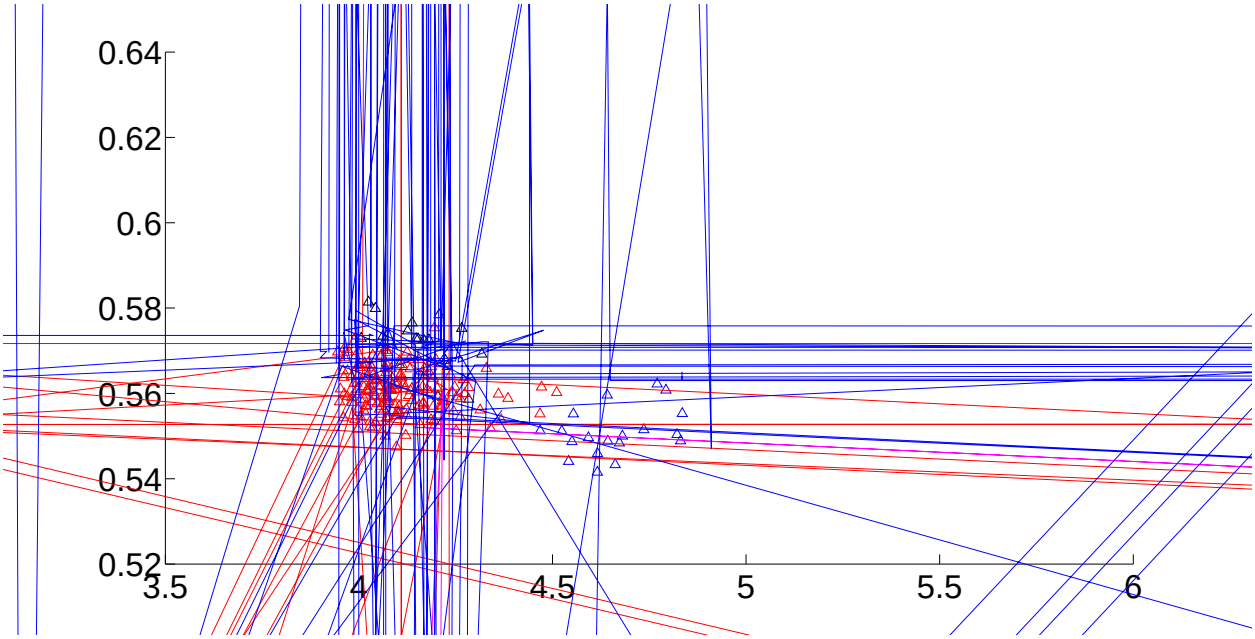
0.64
0.62
0.6
0.58
0.56
0.54
0.52
3.5
4
4.5
5
5.5
6

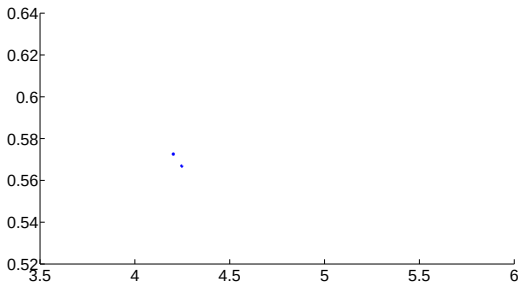
0.64
0.62
0.6
0.58
0.56
0.54
0.52
3.5
4
4.5
5
5.5
6

Doug Saddy, the director, who has provided a huge amount of advice and encouragement; Tamsin Lee who patiently prepared the data sets; Danica Greetham, Jon Ward and other members of the Centre for the Mathematics of Human Behaviour at Reading; Tom Johnstone and Bhisma Chakrabarti who encourage the application of communicability ideas to fMRI data; and our long term collaborator Des Higham, who with Peter Grindrod and others developed the original ideas of communicability as a generalization of centrality for evolving graphs, and who has provided challenge and advice on many occasions.

This work benefited from funding, including the provision of direct support for Zhivko Stoyanov, from a number of EPSRC grants over the last three years: EP/F033036/1, Cognitive Systems Science (Bridging the Gaps); EP/I016856/1, Neuro-Cloud; EP/H024883/1, An integrated neural field computational model; and EP/G065802/1, The Digital Economy HORIZON Hub.

References

References

J. Crofts and D. J. Higham. Googling the brain: Discovering hierarchical and asymmetric network structures, with applications in neuroscience. *Internet Mathematics (Special Issue on Biological Networks)*, 7(4):233–254, 2011.

E. Estrada. *The Structure of Complex Networks: Theory and Applications*. Oxford University Press, 2011. ISBN 9780199591756.

E. Estrada, N. Hatano, and M. Benzi. The physics of communicability in complex networks. *Physics Reports*, 2012. To appear (available on-line).

D. Gfeller and P. De Los Rios. Spectral coarse graining of complex networks. *Phys. Rev. Lett.*, 99(3), 2007. doi: 10.1103/PhysRevLett.99.038701. URL n p o or 1 11 n s ►◄1.

D. Gfeller and P. De Los Rios. Spectral coarse graining and synchronization in oscillator networks. *Phys. Rev. Lett.*, 100(17):174104, May 2008. doi: 10.1103/ / / / / / /

S. Itzkovitz, R. Levitt, N. Kashtan, R. Milo, M. Itzkovitz, and U. Alon. Coarse-graining and self-dissimilarity of complex networks. *Phys. Rev. E Stat. Nonlin. Soft Matter Phys.*, 71(016127), January 2005.

L. Katz. A new status index derived from sociometric analysis. *Psychometrika*, 18:39–43, 1953.

P. J. Mucha, T. Richardson, K. Macon, M. Porter, and J-P. Onnela. Community structure in Time-Dependent, multiscale, and multiplex networks. *Science*, 328(5980): 876–878, May 2010. ISSN 1095-9203. doi: 10.1126/science.1184819. URL n p o or 1 11 s n 11 1 .

Z. Stoyanov, B. Chakrabarti, G. Smith, P. Grindrod, D. Greetham, D. Saddy, T. Lee, and T. Johnstone. High resolution communicability measures of performance across fmri data from human brains. 2013. To be submitted.

V. Tozzini. Coarse-grained models for proteins. *Curr. Opin. Struct. Biol.*, 15(2):144–150, April 2005.